



Al/Ni metal intermetallic composite produced by accumulative roll bonding and reaction annealing

A. Mozaffari, M. Hosseini, H. Danesh Manesh*

Department of Materials Science and Engineering, School of Engineering, Shiraz University, Shiraz, Iran

ARTICLE INFO

Article history:

Received 1 February 2011

Received in revised form 27 July 2011

Accepted 30 July 2011

Available online 4 August 2011

Keywords:

Metal–intermetallic composite

Accumulative roll bonding process

Mechanical properties

ABSTRACT

In this research, Al/Ni multilayers composites were produced by accumulative roll bonding and then annealed at different temperatures and durations. The structure and mechanical properties of the fabricated metal intermetallic composites (MICs) were investigated. Scanning electron microscopy and X-ray diffraction analyses were used to evaluate the structure and composition of the composite. The Al_3Ni intermetallic phase is formed in the Al/Ni interface of the samples annealed at 300 and 400 °C. When the temperature increased to 500 °C, the Al_3Ni_2 phase was formed in the composite structure and grew, while the Al_3Ni and Al phases were simultaneously dissociated. At these conditions, the strength of MIC reached the highest content and was enhanced by increasing time. At 600 °C, the AlNi phase was formed and the mechanical properties of MIC were intensively degraded due to the formation of structural porosities.

© 2011 Elsevier B.V. All rights reserved.

1. Introduction

Aluminum intermetallic compounds are being studied as a structural material for special applications which demand light weight, high thermal stability, corrosion resistance, and good mechanical properties at high temperature [1–4]. Among various intermetallic compounds, Al–Ni based intermetallic compounds seem to be suitable for practical applications in the transportation, aerospace, and similar industries [5]. However, the intrinsic low ductility and low fracture toughness at room temperature confine their application in engineering designs. A main method to compensate the brittleness of intermetallic compounds is the embedding of the intermetallic phases in the ductile matrix materials in the form of particles or laminates [2]. Hereon, when a crack propagates inside the intermetallic phase and reaches the ductile metallic phase, owing to plastic deformation at the crack tip, the crack is blinded. Thus, the useful properties can practically be utilized in a structural material and the ductility of matrix material could avoid its brittle deficiency.

It has been reported that Al/Ni metal intermetallic composites (MICs) have proper properties, such as high strength, resistance against fatigue and creep, good ductility and toughness, corrosion resistance and so on [6–8]. These properties make them suitable for some application, for instance aerospace, transportation and medical. Different methods have been used to produce MICs, including vacuum hot pressing, physical vapor deposition, magnetron

sputtering, direct solidification and so on [3]. Generally, the production methods of MICs directly affect the shape and distribution state of intermetallic phases. Each technique has some specific advantages and disadvantages [3]. Most of them need expensive equipments and complex processes, which limits their usage at commercial and industrial scales. Dimensional limitations and time-consuming fabrication are other main problems for these methods.

Accumulative roll-bonding (ARB) is a severe plastic deformation process to produce nanostructured materials by introducing structural defects such as dislocations inside the material [9]. ARB is the only severe plastic deformation process applicable to produce continuous bulky materials [10]. Rolling in the ARB process is not solely a deformation process but is a bonding process that could lead to a single-body solid material. The ARB process is also applicable in the fabrication of foams and various types of metal matrix composites [11–15]. Recently, the ARB process and subsequent annealing reactions have been used as a new production method of MICs [16,17]. In this technique, complex heat and chemical treatments, such as heat treatment at controlled environment, are not required [18]. Also, simplicity, no dimensional limitations and cheaper primary commodity are the other major advantages of the ARB process for the production of MICs.

To the best of our knowledge, no evaluation has been conducted on the production of Al/Ni MIC by the ARB process. It would be worth mentioning that compared with low-formable Ti alloys usually used for the same applications, this work aims to employ a general forming process (rolling) to fabricate Al/Ni MICs.

In this research, initially Al/Ni metallic composites were fabricated by six ARB cycles of Al and Ni foils. Afterward, the composites

* Corresponding author. Tel.: +98 711 230 7293; fax: +98 711 230 7293.

E-mail address: daneshma@shirazu.ac.ir (H.D. Manesh).

were annealed at different periods and temperatures. Then, the composition, structure, and mechanical properties of the produced MICs were investigated.

2. Experimental procedures

2.1. Materials

The initial materials used in this research were commercial pure Al and Ni alloys having the specifications listed in Table 1.

2.2. Preparation of the initial Al/Ni multilayer composites

To process the initial metallic multilayer composites, Al and Ni foils were degreased in acetone for 30 min and subsequently wire-brushed. Then, six Ni and five Al foils were stacked together. Afterward, the stacked strips were rolled at room temperature to reduce the multilayer total thickness from 1.1 mm to 0.7 mm. Then, the initial rolled stacks were cut into two equal pieces in length, degreased, scratch brushed and stacked for the ARB process.

ARB of the initial Al/Ni sandwich stack comprised of two main steps: firstly, the surface was degreased in acetone, dried in air and then wire brushed. Secondly, the stacked sandwich samples was concurrently rolled by a 170 mm diameter roll mill at a 15 rpm rolling speed which was repeated six times at room temperature without any lubrication. Cold roll bonding was applied under the condition where the thickness reduction per cycle of the ARB process was 50% ($\varepsilon = 0.8/\text{cycle}$), while for the primary sandwiches ε was 0.5.

2.3. Heat treatment regime

The produced metallic multilayer composites were heat treated at a calibrated electrical furnace at 300, 400, 500 and 600 °C at four different durations including 30, 40, 50 and 60 min. Totally, the sixteen regimes of the heat treatment procedure were used.

2.4. Thermal analyses

The phase formation and heat of reactions were investigated by differential scanning calorimetry (DSC) in a nitrogen atmosphere. The samples were small discs (10 mg) of the primary composite and heated in the temperature range of 100–620 °C at a constant rate of 20 °C/min. The base line was achieved by the repetition of the thermal cycle and to normalize, the base line was eliminated from total heat flow.

2.5. Structural evaluation

The cross-section of the produced composites was prepared for the evaluation of their structure by scanning electron microscope (SEM). The thicknesses of the phases were evaluated perpendicular to the rolling direction drawn at several random positions and the average size of 150–200 layers was measured each time. In the metallography stage, the samples were grounded and polished by 1 μm diamond paste in the last polishing step. The chemical compositions gradient of the interface of the layers were determined by an EDX spectrometer and corrected by ZAF factor using Link ISIS software and calibrated using pure Ni and Al standards.

2.6. X-ray diffraction analysis

In order to identify the phases, the X-ray diffraction technique was used in the cross section of the heat treated composites. Diffraction patterns were recorded using a Philips X'Pert diffractometer employing $\text{Cu K}\alpha$ at the room temperature. The data were collected for the diffraction angles of $10^\circ \leq 2\theta \leq 105^\circ$, with a step width of 0.05° and a step time of 2 s. The phases were determined using the X'pert software.

2.7. Mechanical properties

Tensile tests were carried out by an Instron testing machine at room temperature at a strain rate of $8.3 \times 10^{-4} \text{ s}^{-1}$. The tensile test samples were prepared according to one fifth of the JIS-5 standard dimensions, oriented along the rolling direction. The gauge length and the width of the tensile test specimens were 10 and 5 mm, respectively.

3. Results and discussion

3.1. Structure

The structural and mechanical properties of the initial Al/Ni metallic composite produced by six ARB cycles were investigated in the previous study [15]. Fig. 1 shows the SEM micrograph of the initial non heat-treated Al/Ni composite. In order to specify the proper

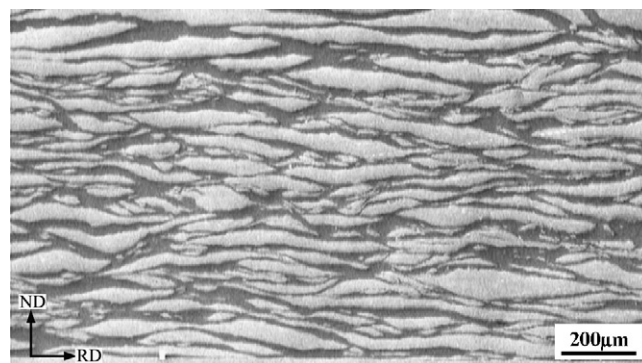


Fig. 1. SEM micrograph of the initial Al/Ni metallic composite after six ARB cycles.

heat treatment regime to produce MICs, it is essential to determine the formation temperatures of intermetallic compounds. DSC analyses were conducted for this purpose. Fig. 2 shows the result of the DSC experiment. As it can be seen, there exist four peaks. Each peak shows an exothermic reaction. Owing to the presence of peaks in the ranges of 300–400, 400–500 and 500–600 °C, the borders of these ranges were selected as the annealing temperatures.

Fig. 3a shows the XRD patterns of the non-heat treated and the samples annealed at 300 °C. The only intermetallic phase which is present in this annealing temperature and both the durations is Al_3Ni . The interface structures of Al/Ni annealed at 300 °C for different times are illustrated in Fig. 4. As it can be seen, initially the intermetallic phase is nucleated at the Al/Ni interface (Fig. 4a). By increasing time, the new intermetallic phase islands grow along interface (Fig. 4b) to form a relatively uniform layer on the interface (Fig. 4c). Finally, the intermetallic phase growths perpendicular to the interface (Fig. 4d). Previously, Coffey et al. [19] obtained the similar result in the fabrication of Al-rich phase in the Al/metal multilayers during the annealing process.

The development of nucleation at the initial interface plane broadens the DSC peaks. As it can be seen in Fig. 2, the Al_3Ni peak consists of two adjacent peaks. The first peak (at 305 °C) is correspond to the lateral growth and the second peak (at 320 °C) is referred to the perpendicular growth of the Al_3Ni intermetallic phase, as schematically illustrated in Fig. 2.

Fig. 5 shows the SEM images of the Al/Ni multilayers annealed at 400 °C at the different periods. In the similar way to the previ-

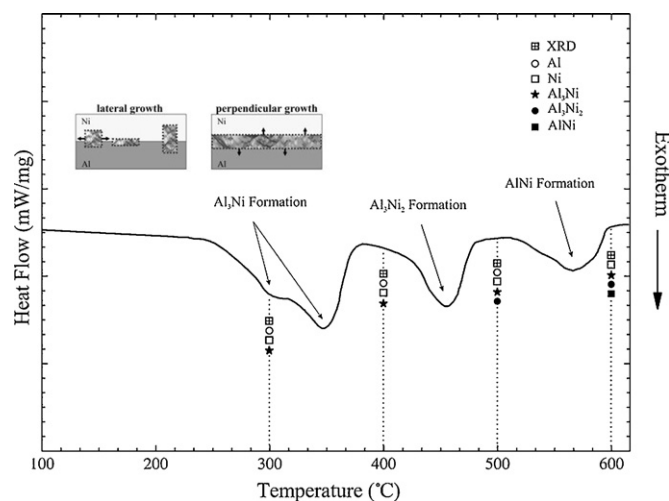


Fig. 2. DSC curve of the ARBed Al/Ni multilayer sample. Schematic illustration of the Al_3Ni growth stages and the present phases at each temperature resulted by the XRD analyses are also being shown.

Table 1
Specifications of the Al and Ni foils.

Materials	Chemical composition (wt.%)	Sheet dimensions (L, W, t) (mm × mm × mm)	Hardness (VHN)	Elongation (%)	Yield strength (MPa)
Al (1060)	99.5 Al, 0.20 Si, 0.25 Fe, 0.05 Cu	120 × 60 × 0.1	27	13.2	34.7
Ni (200 series)	99.6 Ni, 0.3 Mn, 0.05 Si, 0.05 Fe	120 × 60 × 0.1	81	9.8	126.4

ous annealing temperature, an intermetallic phase is formed in the Al/Ni interfaces and grows by time. Corresponding to the DSC result (Fig. 2), the XRD analysis shows that at 400 °C the only existing intermetallic phase likewise is Al_3Ni (Fig. 3b). Fig. 6a quantitatively shows the increment in the thickness of the Al_3Ni phase by increasing the annealing time at 300 and 400 °C. The higher thickness of the Al_3Ni layers in the identical time at 400 °C is due to higher diffusion and growth rate.

The XRD patterns of the samples annealed at 500 °C for 30 and 60 min are showed in Fig. 3c. The peaks of the Al_3Ni_2 intermetallic phase are also shown together with Al, Ni and the Al_3Ni peaks at 30 min. Also, at the heating period of 60 min, the peaks of the Al phase are relatively not present. The SEM images of the multilayers annealed at 500 °C for the different periods are shown in

Fig. 7. In the SEM images, the formation of the new intermetallic phase is obvious and distinguishable by a different color. As it can be seen, the Al_3Ni_2 phase is formed at the interface of the Al_3Ni and Ni phases. Furthermore, after 50 min, the Al phase is dissociated completely, which corresponds to the XRD result. These images indicate that the increment in the heat treatment period leads to the simultaneous consumption and the production of the Al_3Ni and Al_3Ni_2 phases, respectively. Fig. 6b quantifies the thickness of each intermetallic layer as well as their total thickness.

Fig. 3d displays the XRD pattern of Al/Ni multilayer heat treated at 600 °C for 30 and 60 min. At this temperature, the peaks of the AlNi intermetallic phase are also revealed besides the Al_3Ni , Al_3Ni_2 and Ni phases peaks. Also, the peaks of the Al phase obliterated in both the period. The EDX analyses also confirm the presence of

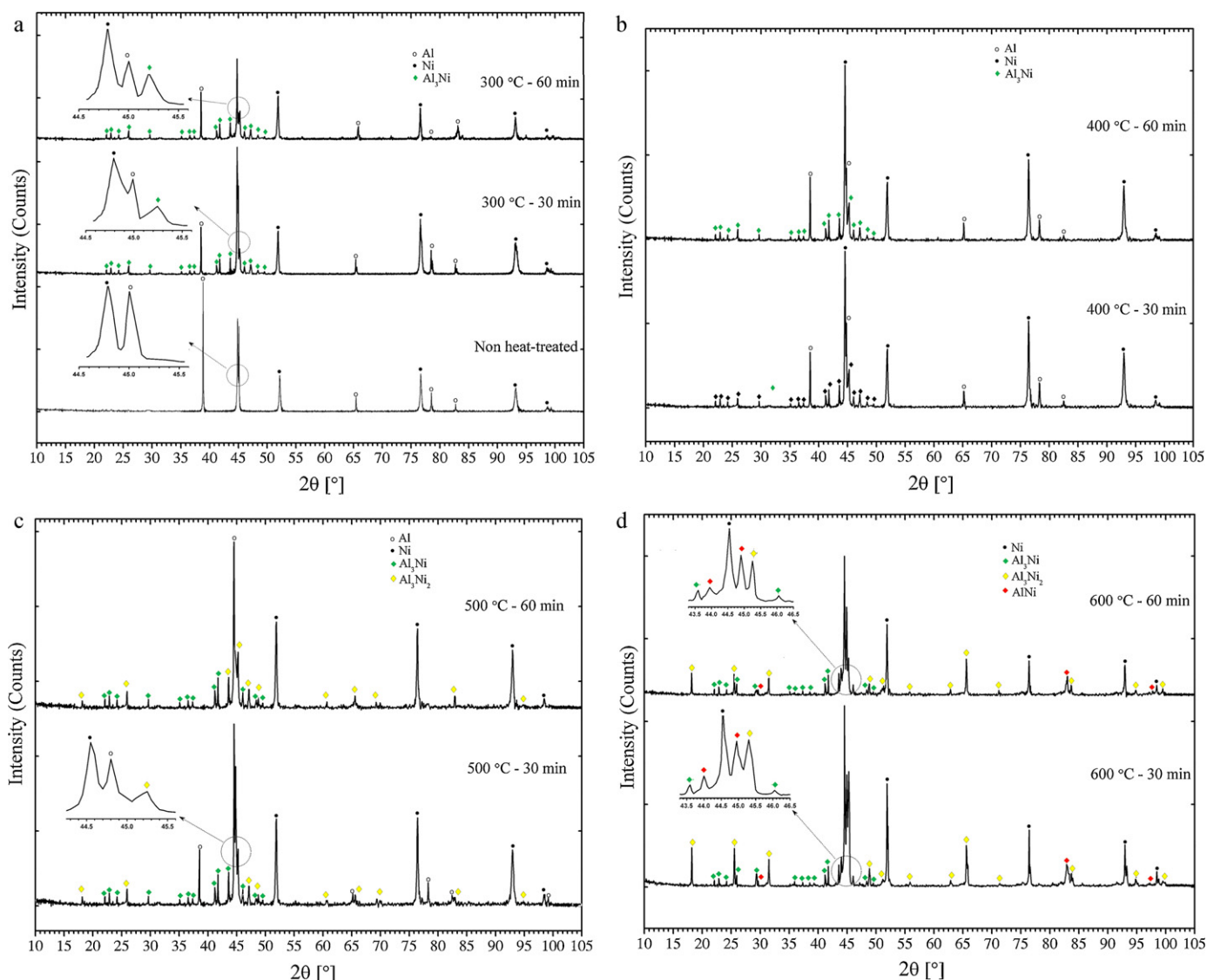


Fig. 3. XRD patterns of the samples annealed for 30 and 60 min at (a) 300 °C and also non heat-treated Al/Ni multilayer composite, (b) 400 °C, (c) 500 °C and (d) 600 °C.

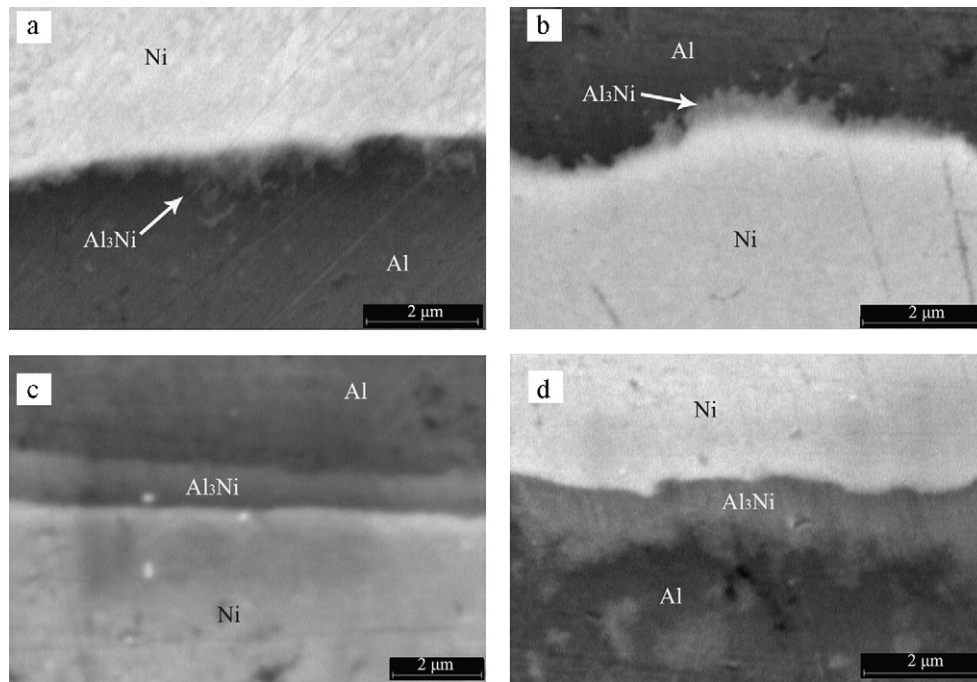


Fig. 4. SEM images of the samples annealed at 300 °C for (a) 30 min, (b) 40 min, (c) 50 min and (d) 60 min.

the Al_3Ni , Al_3Ni_2 and AlNi phases in the composite structure at this temperature (Fig. 8). As it can be seen, the AlNi phase grows in the $\text{Ni}/\text{Al}_3\text{Ni}_2$ interface.

Generally, in different methods in which Al/Ni multilayers are used for the fabrication of intermetallic phases, the Al_3Ni is the first produced phase [20]. The reason is the difference in the diffusion coefficient of Al and Ni atoms, in such a way that the diffusion of Ni atoms in the Al substrate is higher than the vice versa condition [20]. It is due to the lower atomic radius of Ni atoms. Nevertheless, based on the nominal composition of the multilayer and the process

type, other primary phases such as AlNi , AlNi_3 and even Al_9Ni_2 metastable phase has been reported [18]. The former difference is due to the concentration gradient imposed before the annealing stage [21]. When the time and/or temperature of the heat treatment process increase, from the rich side of the Al element in the $\text{Al}-\text{Ni}$ phase diagram, various intermetallic phases are formed gradually.

The SEM images of the samples at the four annealing periods at 600 °C are shown in Fig. 9. As shown in this figure, due to the fully consumption of the Al phase and also high activation energy for diffusion in the intermetallic phases, when the annealing

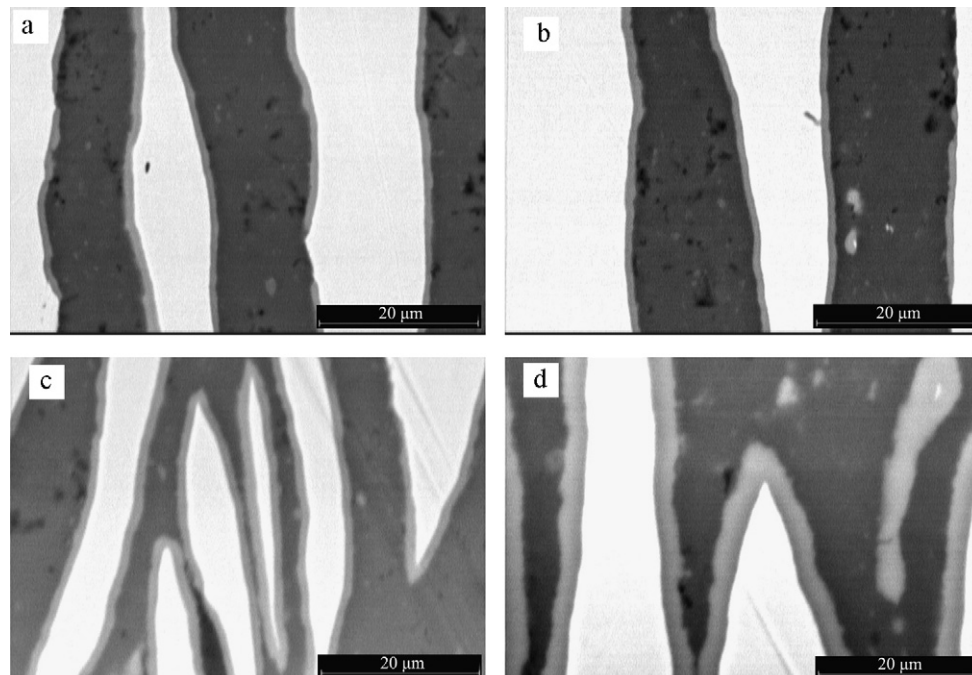


Fig. 5. SEM images of the samples annealed at 400 °C for (a) 30 min, (b) 40 min, (c) 50 min and (d) 60 min.

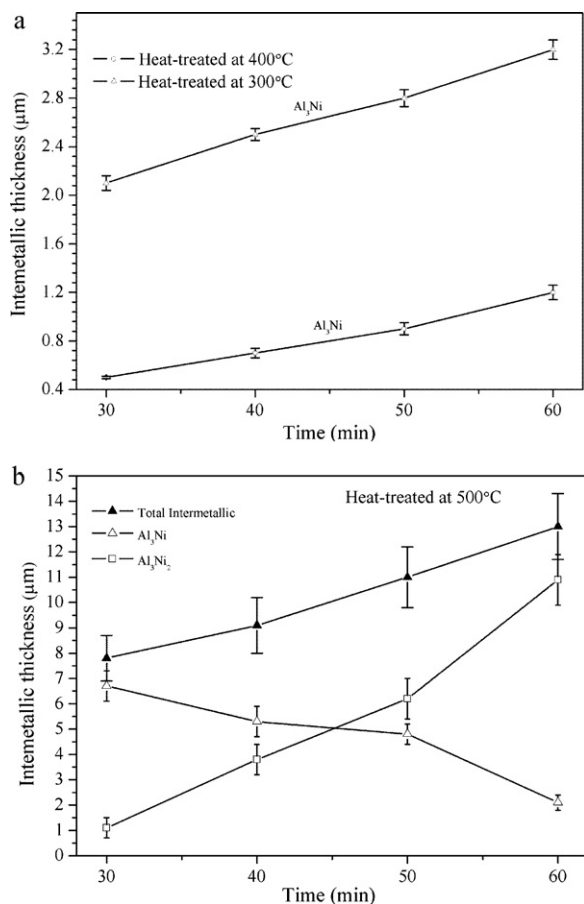


Fig. 6. Changes in the thickness of the intermetallic phases when the annealing period increases at the annealing temperatures of (a) 300 and 400 °C and (b) 500 °C.

time increases, the total thickness of the intermetallic layers is not approximately changed. However, the thickness of a phase is altered and the intermetallic phases are transformed to each other, in such a way that the Al_3Ni phase is dissociated and the two other intermetallic phases grow. As it can be seen, porosities are created in the composite structure at this annealing temperature and grow by progression of annealing (Fig. 9e). The quantitative measurements of the layers thickness at this condition are too difficult because of the porosities presence. It can be seen that the thickness of the $AlNi$ layer is approximately narrow (Fig. 8).

The simultaneous occurrence of several phenomena is responsible for the porosity formation. Owing to the vacancies diffusion toward the interface, the Kirkendall voids are formed and the bonding decreases in this zone [16]. Also, the crystal structure of the intermetallic phases is more compact with respect to Al and Ni metals. Consequently, the volume changes during the intermetallic phase formation cause the residual stress [4]. This effect and the dissimilar contraction behavior of the Al_3Ni and Al_3Ni_2 phases during the cooling period [22] create cracks and voids between some layers.

3.2. Mechanical properties

Fig. 10 shows the total elongation (TE) of the Al/Ni multilayer composites heat treated at the different durations and temperatures in comparison with the initial metallic composite. Considering Fig. 10, the composites annealed at 300 °C show higher TE (at the same heat treating period) with respect to the other samples. Moreover, TE is enhanced more than 17% by increasing the annealing time from 30 min to 60 min. The changes in the engineering yield strength (YS) and tensile strength (TS) of these samples are also illustrated in Fig. 11. With attention to Fig. 11, YS and TS of these composites decrease when the annealing time increases. The samples annealed at 400 °C have middle values of TE, YS and TS. In contrast to the samples annealed at 300 °C, TE decreases, but YS and TS increase when annealing prolongs. At the same annealing times, TE is reduced approximately 1.25 units, but YS is increased

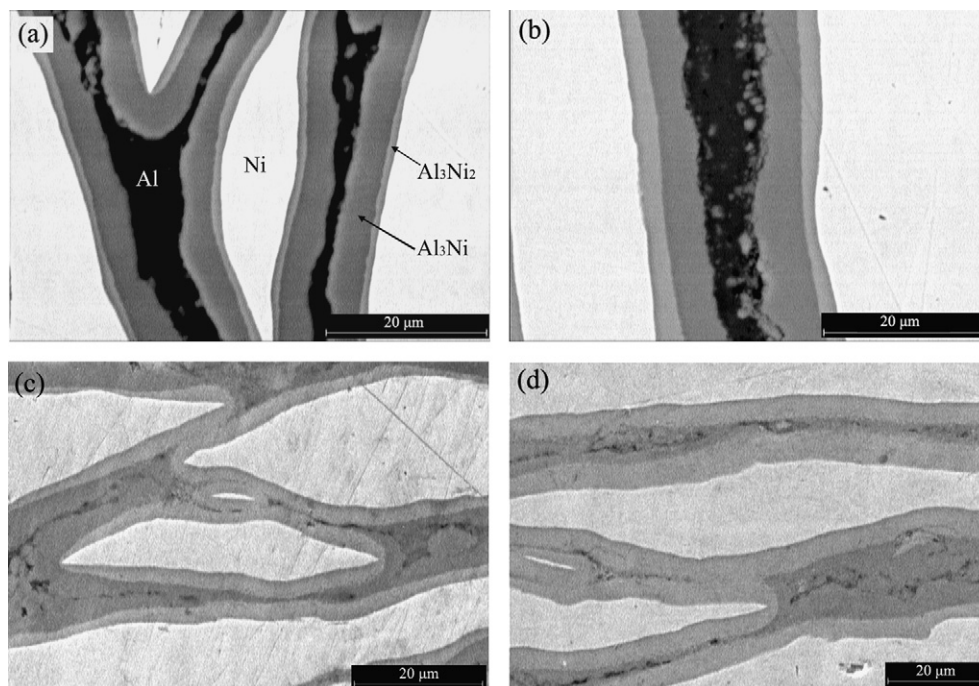


Fig. 7. SEM images of the samples annealed at 500 °C for (a) 30 min, (b) 40 min, (c) 50 min and (d) 60 min.

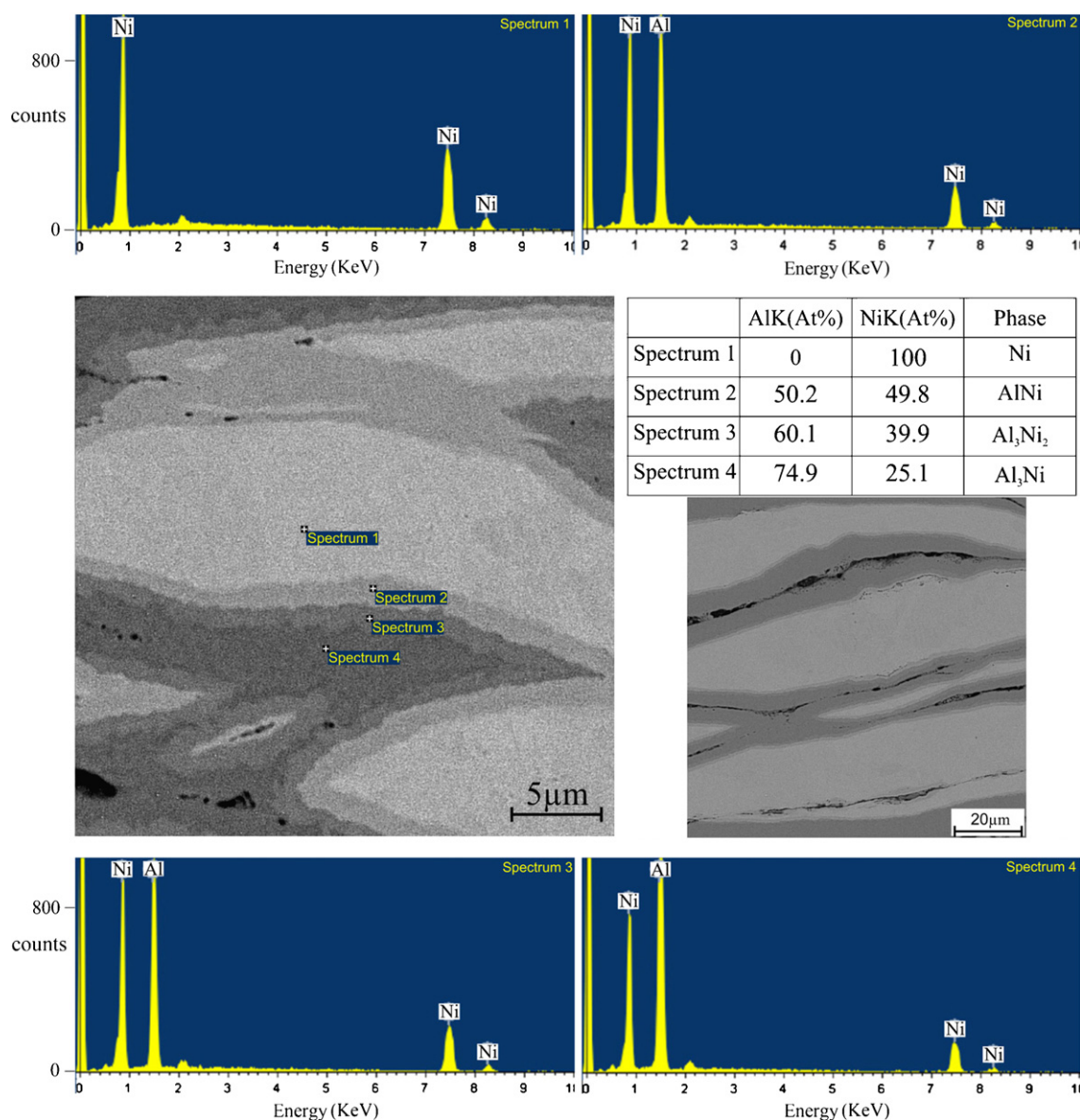


Fig. 8. EDX spectra across the structural layers of MIC.

nearly 22 MPa at all the annealing times and TS is enhanced 20, 36, 50 and 48 MPa at 30, 40, 50 and 60 min annealing period, when the annealing temperature is raised from 400 °C to 500 °C. The samples annealed at 500 °C show the maximum YS and TS at all the periods. Especially at 60 min, 340 and 445 MPa were obtained for YS and TS respectively. As indicated in Figs. 10 and 11, the minimum TE coincides with the minimum TS and YS at the annealing temperature of 600 °C. TE, TS and YS decrease continuously with increasing the annealing time. Quantitatively, when annealing is prolonged from 30 min to 60 min, TE, TS and YS decrease 38%, 37% and 30% respectively.

Hereon, two factors play a main role in the evolution of the mechanical properties. First, the recrystallization of the initial Al and Ni phases leads to the decrement of the strength and the enhancement of TE of the composite. In this case, the Al phase usually has a more important role because of its continuity and its function as a matrix material. The second factor is the formation of the intermetallic phases. The presence of these phases increases the strength and decreases TE of the composites, due to their intrinsic high strength and low toughness [23]. On the other hand, the severe

plastic deformation of the initial composite results in a reduction in the recrystallization temperatures of the Al and Ni phases, owing to the high quantity of microstructural defects and the thermal instability of severe plastic deformed materials [24]. Generally, Al and Ni metals are recrystallized at ~200 and 600 °C, respectively (based on the half of their standard melting points). Considering the reduction of the recrystallization temperature, the Ni phase is still recrystallized at a temperature in which the composite structure mainly includes the intermetallic phases. Therefore, at high annealing temperatures the continuity of the high strength intermetallic phases reduces the effect of the Ni phase recrystallization on the mechanical properties of the composite. Owing to the low recrystallization temperature of the Al phase, the low volume fraction of the intermetallic phases at low temperatures and also the continuity of the Al phase, the influence of this phase at the low annealing temperatures is more.

Based on the previous statements, at 300 °C, the recrystallization of the Al phase is the main cause of the increment in TE and the decrement in YS and TS of MICs. At this temperature, the relatively low volume fraction (low thickness) of the produced Al₃Ni

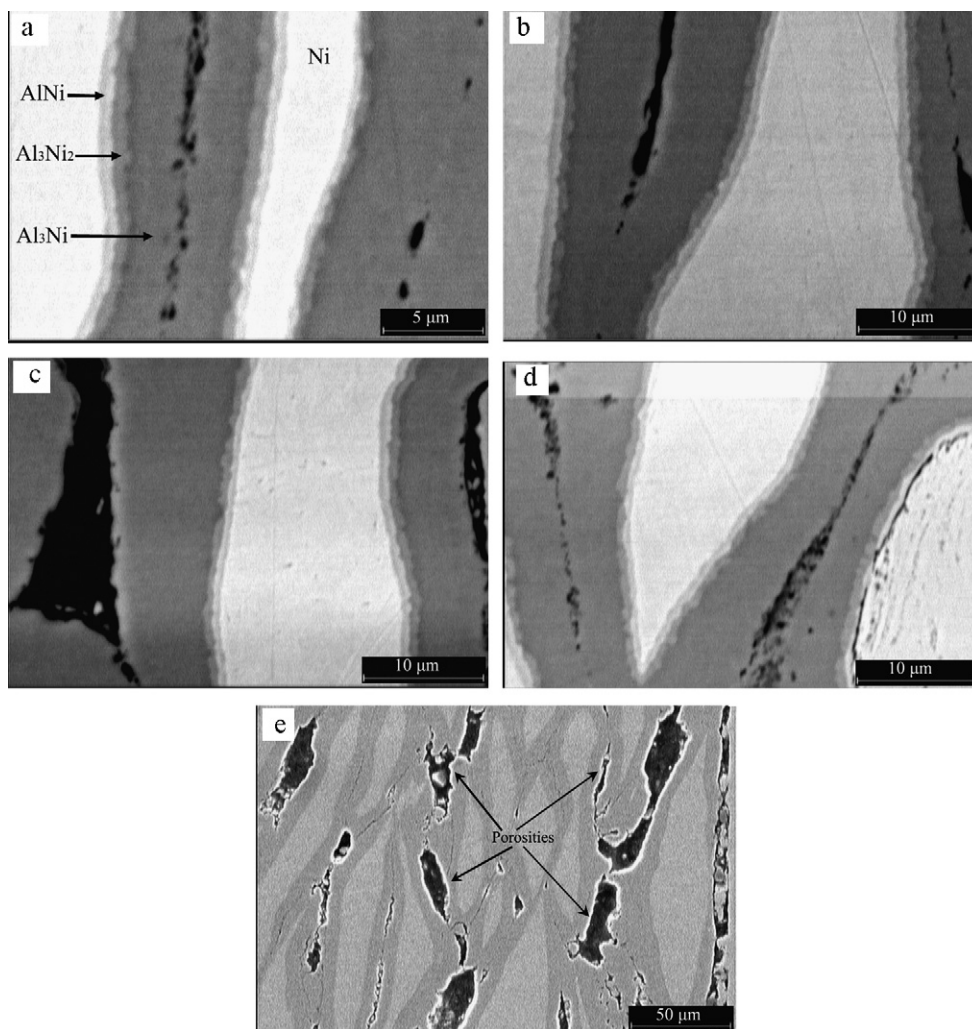


Fig. 9. SEM images of the samples annealed at 600 °C for (a) 30 min, (b) 40 min, (c) 50 min, (d) 60 min and (e) porosities formed in the sample.

intermetallic phase cannot compensate the recrystallization softening (Fig. 6a). When the annealing temperature increases to 400 and 500 °C, the increment in the thickness of the intermetallic layer(s) can compensate the recrystallization softening of the Al

phase. As a consequence, TS and YS of the composites are enhanced and TE decreases. At 500 °C, the harder Al_3Ni_2 phase is added to the MIC structure [2]. Its crystal structure is more compact ($p3m1$ space group in comparison to $pnma$ space group of Al_3Ni) [25]. This lowers the dislocation mobility inside the Al_3Ni_2 phase, leading to more strengthening in composite. When the volume fraction of the Al_3Ni_2 phase increases and the Al phase is completely

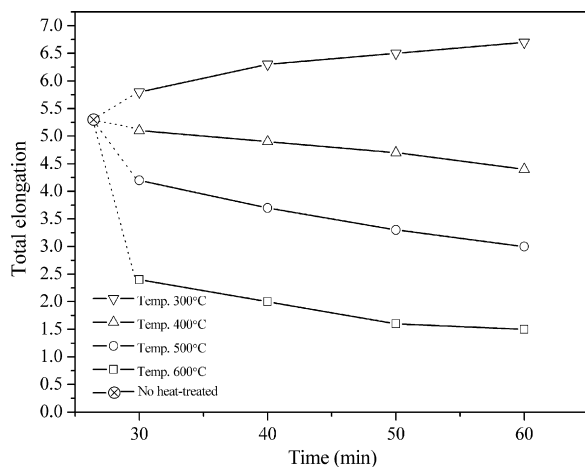


Fig. 10. Total elongation of MIC at the different annealing times and temperatures with respect to the initially ARBed metallic composite.

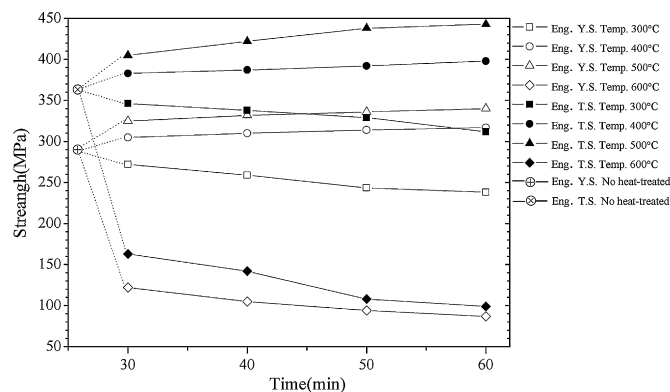


Fig. 11. Tensile and yield strength of MIC produced at the different annealing regimes in comparison with the ARBed non-heat treated sample.

consumed at 500 °C, the formation of the continuous intermetallic phases results in the decrement in TE and the increment in YS and TS of MICs with respect to the composites annealed at 400 °C. At the annealing temperature of 600 °C, the development of the structural porosities as a crack (Fig. 9e) leads to a crucial reduction in the mechanical properties in terms of TE, YS and TS.

4. Conclusions

According to the results of this research, accumulative roll bonding followed by annealing is a suitable process to process Al–Ni metal intermetallic composite. At the annealing temperature of 300 °C, the Al₃Ni phase is formed in the Al/Ni interface in two stages by progression of annealing. Firstly, the intermetallic phase is nucleated in preferential locations and grows along the interface. Secondly, the Al₃Ni islands coalesce and subsequently grow perpendicular to the interface. The occurrence of the Al matrix recrystallization softening, as a dominant mechanism in the annealing stage results in the increase in TE and the decrement in TS and YS of the composites. When the annealing temperature increases to 400 °C, the increment in the thickness of the high strength intermetallic layer reduces TE and is enhanced TS and YS of MICs. At 500 °C, the harder Al₃Ni₂ phase is added to the structure of MICs and the volume fraction of the intermetallic phases increases. Therefore, TE decreases and the strengths increase with respect to the samples heat treated at 400 °C. The AlNi phase was produced at 600 °C and grown by time; however, the formation of the porosities at this temperature leads to the intensive reduction in the mechanical properties. Consequently, the highest increment in the strength of the metallic composite is obtained at the annealing temperature of 500 °C.

Acknowledgment

The authors would like to thank the research board of Shiraz University for the financial support and provision of research facilities used in this work.

References

- [1] Y. Lu, M. Hirohashi, J. Mater. Sci. 18 (1999) 395–398.
- [2] L. Ke, C. Huang, L. Xing, K. Huang, J. Alloys Compd. 503 (2010) 494–499.
- [3] Z. Xia, J. Liu, S. Zhu, Y. Zhao, J. Mater. Sci. 34 (1999) 3731–3735.
- [4] T. Li, E. Al Olevsky, M.A. Meyers, Mater. Sci. Eng. A 348 (2007) 207–212.
- [5] R.J. Herbert, J.H. Perepezko, Scr. Mater. 50 (2004) 807–812.
- [6] S.K. Pabi, B.S. Murty, Mater. Sci. Eng. A 214 (1996) 146–152.
- [7] T.R. Smith, Mater. Res. Soc. Symp. 350 (1994) 219–224.
- [8] T.P.D. Rajan, R.M. Pillai, B.C. Pai, J. Alloys Compd. 453 (2008) L4–L7.
- [9] M. Hosseini, H. Danesh Manesh, Mater. Des. 31 (2010) 4786–4791.
- [10] K. Wu, H. Chang, E. Maawad, W.M. Gan, H.G. Brokmeier, M.Y. Zheng, Mater. Sci. Eng. A 527 (2010) 3073–3078.
- [11] K. Kitazono, E. Sato, K. Kuribayashi, Scr. Mater. 50 (2004) 495–498.
- [12] M. Alizadeh, M.H. Paydar, J. Alloys Compd. 492 (2010) 231–235.
- [13] L. Ghalandari, M.M. Moshksar, J. Alloys Compd. 506 (2010) 172–178.
- [14] Y.F. Sun, N. Tsuji, H. Fujii, F.S. Li, J. Alloys Compd. 504 (2010) S443–S447.
- [15] A. Mozaffari, H. Danesh Manesh, K. Janghorban, J. Alloys Compd. 489 (2010) 103–109.
- [16] R. Zhang, V.L. Acoff, Mater. Sci. Eng. A 463 (2007) 67–73.
- [17] D. Yang, P. Hodgson, C. Wen, Intermetallics 17 (2009) 727–732.
- [18] L.M. Peng, J.H. Wang, H. Li, J.H. Zhao, L.H. He, Scr. Mater. 52 (2005) 243–248.
- [19] K.R. Coffey, L.A. Clevenger, K. Barmak, D.A. Rudman, C.V. Thompson, Appl. Phys. Lett. 55 (1989) 9–14.
- [20] X. Sauvage, G.P. Dinda, G. Wilde, Scr. Mater. 56 (2007) 181–184.
- [21] K.J. Blobaum, D. Van Heerden, A.J. Gavens, T.P. Weihs, Acta Mater. 51 (2003) 3871–3884.
- [22] M.C. Chen, H.C. Hsieh, W. Wu, J. Alloys Compd. 416 (2006) 169–172.
- [23] P.F. Thomason, G. Rauchs, P.J. Withers, Acta Mater. 50 (2002) 1453–1466.
- [24] Y. Sun, H. Fujii, Y. Takada, N. Tsuji, K. Nakata, K. Nogi, Mater. Sci. Eng. A 527 (2009) 317–321.
- [25] D. Shi, B. Wen, R. Melnik, S. Yao, T. Li, J. Solid State Chem. 182 (2009) 2664–2669.